RiESTech
Recent in Engineering Science and Technology

MBI

Article

Enhancing Proton Exchange Membrane Fuel Cell (PEMFC) Performance through Optimized Design of Parallel Channel Bipolar Plates

Moh Nurkhamal [1], Vika Rizkia [1,*], Vina Nanda Garjati [1], and Radhi Maladzi [1]

[1] Jurusan Teknik Mesin, Politeknik Negeri Jakarta, Jl. Prof. G. A. Siwabessy, Kampus UI, Depok, 16425.
* Correspondence: vika.rizkia@mesin.pnj.ac.id

Abstract: In this modern era, the demand for efficient and environmentally friendly energy sources is increasing. One technology with significant potential to meet this demand is the Proton Exchange Membrane Fuel Cell (PEMFC). This study aims to investigate the influence of channel width and depth variations in parallel bipolar plate designs on PEMFC performance. Computational Fluid Dynamics (CFD) was employed to analyze hydrogen flow distribution and pressure across various design variations. The results demonstrate that channel width and depth significantly affect pressure distribution and flow velocity, which in turn influence the efficiency of the PEMFC system. Increasing channel width generally reduces maximum pressure, while deeper channels help to distribute pressure more evenly across the bipolar plate. Optimized channel width and depth can enhance PEMFC operational performance by reducing pressure drop and promoting uniform flow distribution.

Keywords: PEMFC; Bipolar Plate; CFD; Pressure Drop; Flow Distribution

Citation:. Nurkhamal, M.; Rizkia, V.; Garjati, V. N.; Maladzi, R. (2025). Enhancing Proton Exchange Membrane Fuel Cell (PEMFC) Performance through Optimized Design of Parallel Channel Bipolar Plates. Recent in Engineering Science and Technology, 3(01), 42–57. Retrieved from https://www.mbi-journals.com /index.php/riestech/article/view/94

Academic Editor: Iwan Susanto

Received: 29 January 2025
Accepted: 30 January 2025
Published: 31 January 2025

1. Introduction

Hydrogen, as an abundant element in the universe, plays a crucial role in decarbonization efforts. Its potential as an environmentally friendly energy source can reduce carbon emissions and replace fossil fuels[1]. Technologies like fuel cells, which utilize hydrogen and oxygen to generate electricity, enable clean energy utilization in various applications, including electric vehicles, power plants, and spacecraft[2–4].

Proton Exchange Membrane Fuel Cells (PEMFCs) are widely employed in vehicles[5]. These devices comprise Membrane Electrode Assemblies (MEA), Gas Diffusion Layers (GDL), and bipolar plates[6]. Among these components, bipolar plates play a critical role in PEMFC stacks, including separating the cathode and anode, distributing reactant gases, and conducting electrons[7].

The flow field design on bipolar plates ensures uniform distribution of reactant gases, provides structural support for the MEA, and facilitates water and heat management. An appropriate flow field design can enhance PEMFC performance and reduce costs by up to 50%[8].

Parallel flow field designs are commonly used due to their ease of fabrication, cost-effectiveness, and lower pressure drop compared to other designs. However, this type exhibits relatively low velocity and uneven reactant gas distribution (maldistribution), leading to a high risk of water accumulation[9,10]. This issue disrupts gas distribution along the flow field, ultimately hindering PEMFC performance.

Previous research has proposed modifications and analyzed the causes of flow maldistribution in parallel designs using geometric variations. Some studies highlight the importance of inlet and outlet orientation, which can result in preferential flow and cell malfunction. Additionally, these studies emphasize the significance of barrier or rib positioning and rib shape in bipolar plate channels[11–13]. Other research indicates that the location of inlets and outlets at the ends of parallel plates can lead to low channel velocities and inadequate water removal[14].

Numerous studies have explored adaptive and varied designs to address current bipolar plate limitations and optimize PEMFC performance and efficiency. However, research specifically investigating the impact of bipolar plate modifications on parallel designs, considering channel width and depth to enhance flow rate and minimize hydrogen pressure drop in PEMFCs, remains limited. Consequently, further research in this area is crucial in Indonesia.

This research gap is particularly crucial for Indonesia, a country with abundant renewable energy resources and a growing interest in fuel cell technology. Developing efficient and cost-effective PEMFCs can contribute significantly to Indonesia's efforts to reduce reliance on fossil fuels and transition towards cleaner energy sources.

This study explores various approaches to overcome the limitations of conventional parallel designs. One approach involves geometric modifications combining parallel and serpentine characteristics, along with adaptations in dimensional variations. The aim is to investigate how channel width and depth influence flow within geometrically modified parallel bipolar plates. The methodology includes Computational Fluid Dynamics (CFD) using Ansys Fluent Simulation to model gas flow into the modified bipolar plate design, considering variations in channel depth and width. The objective is to predict locations of flow rate and pressure drop, as well as interactions with the resulting flow patterns. Subsequently, design variations will be analyzed and compared to evaluate their impact on gas flow distribution and pressure drop, ensuring uniform reactant gas distribution and reducing water accumulation. This research aims to investigate the influence of channel width and depth variations in parallel bipolar plate designs on PEMFC performance.

2. Materials and Experiment Methods

This study modifies the parallel flow field design on PEMFC bipolar plates to achieve uniform hydrogen gas distribution and optimal flow velocity. The modifications investigated involve variations in channel width and depth, as detailed in Table 1.

Table 1. Modified Parallel Flow Field Designs

Code	Channel width (mm)	Channel Depth (mm)
PRL1	0.5	0.6
PRL2	0.5	0.7
PRL3	0.5	0.9
PRL4	0.7	0.6
PRL5	0.7	0.7
PRL6	0.7	0.9
PRL7	1	0.6
PRL8	1	0.7
PRL9	1	0.9

The 3D designs were created using SolidWorks software. Subsequently, design variations were simulated using Ansys Fluent R2 2024 to analyze the influence of channel depth and width on flow velocity, pressure drop, and hydrogen gas distribution.

The steps involved in conducting the CFD simulations using Ansys Fluent are as follows:

1. Open Ansys 2024 software within the Workbench 2024 application.
2. Set the unit system to comply with International Standard units.
3. Select the Ansys Fluent feature.
4. Import the 3D design, created in STEP format, into the Geometry interface.
5. Utilize the "extract volume" setting on the imported 3D design to define the hydrogen flow channels for analysis.
6. Generate a mesh for the channel geometry
7. Once the mesh exhibits a structured visual representation and adequately captures critical regions, the subsequent step involves setting up the simulation. This stage encompasses specifying the fluid flow type, fluid material properties, boundary conditions, initialization parameters, and running the simulation.

Data analysis in this study employs Computational Fluid Dynamics (CFD). CFD enables in-depth analysis of fluid flow, including pressure distribution and flow velocity, within the parallel bipolar plate design.

3. Results and Discussion

3.1. Determining Hydraulic Diameter and Reynolds Number

Hydraulic diameter and Reynolds number are crucial parameters in characterizing fluid flow behavior within the bipolar plate channels. The hydraulic diameter (Dh) represents the effective cross-sectional area available for flow, while the Reynolds number (Re) predicts the flow regime (laminar or turbulent).

The hydraulic diameter for rectangular channels is calculated using the formula:

$$D_h = \frac{2ab}{a+b} \qquad (1)$$

D_h = hydraulic diameter

a = The Channel width

b = The Channel depth

The Reynolds number is determined by:

$$Re = (ϱ * v * Dh) / μ \qquad (2)$$

where:

- ϱ is the density of hydrogen gas
- v is the flow velocity
- Dh is the hydraulic diameter
- μ is the dynamic viscosity of hydrogen gas

The Reynolds number will be derived based on the properties of the fluid under investigation. In this study, the properties of hydrogen gas were obtained from the Ansys software, as depicted in Figure 1.

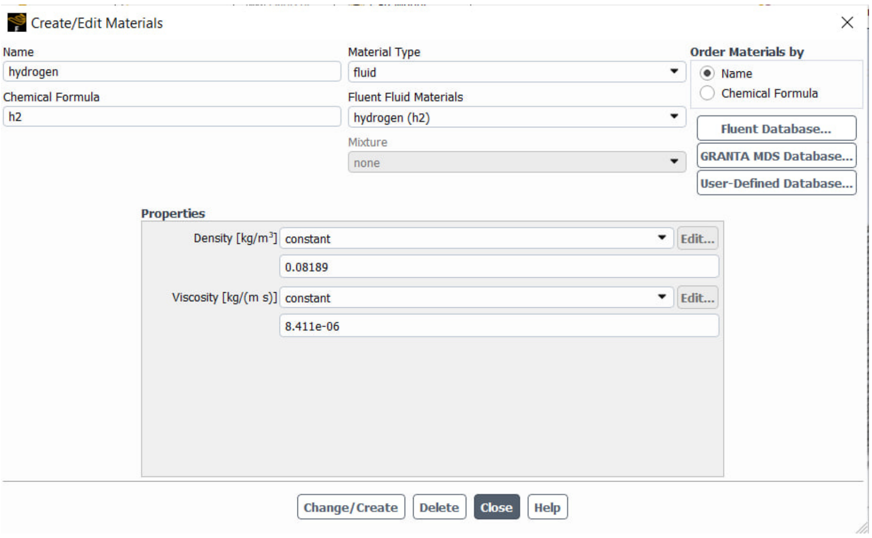

Create/Edit Materials

Name: hydrogen

Chemical Formula: h2

Material Type: fluid

Fluent Fluid Materials: hydrogen (h2)

Mixture: none

Order Materials by: ● Name ○ Chemical Formula

Properties

Density [kg/m^3]: constant, 0.08189

Viscosity [kg/(m s)]: constant, 8.411e-06

Figure 1. Hydrogen Gas Properties in Ansys Software

Table 2. Calculated hydraulic diameter and Reynolds number for all variables

Code	hydraulic diameter (mm)	Reynolds number
PRL1	0.545	63.5
PRL2	0.583	67.91
PRL3	0.642	74.84
PRL4	0.646	75.19
PRL5	0.7	81.37
PRL6	0.788	91.43
PRL7	0.75	87.19
PRL8	0.824	95.67
PRL9	0.947	109.86

The calculation of hydraulic diameter and Reynolds number are presented in Table 2. Based on the obtained Reynolds numbers and the criteria outlined in Table 2, the type of flow that needs to be incorporated into the CFD analysis is laminar flow, as all calculated Reynolds numbers are below 2000.

3.2. Hydrogen Flow Pressure Analysis using Computational Fluid Dynamics (CFD) Simulation

This section presents the findings obtained from the CFD simulations conducted using Ansys Fluent. The analysis focuses on the impact of channel width and depth variations on key parameters such as hydrogen flow pressure and velocity within the modified bipolar plate designs. Figure 2 illustrates the influence of channel width and depth variations on hydrogen flow pressure in this study.

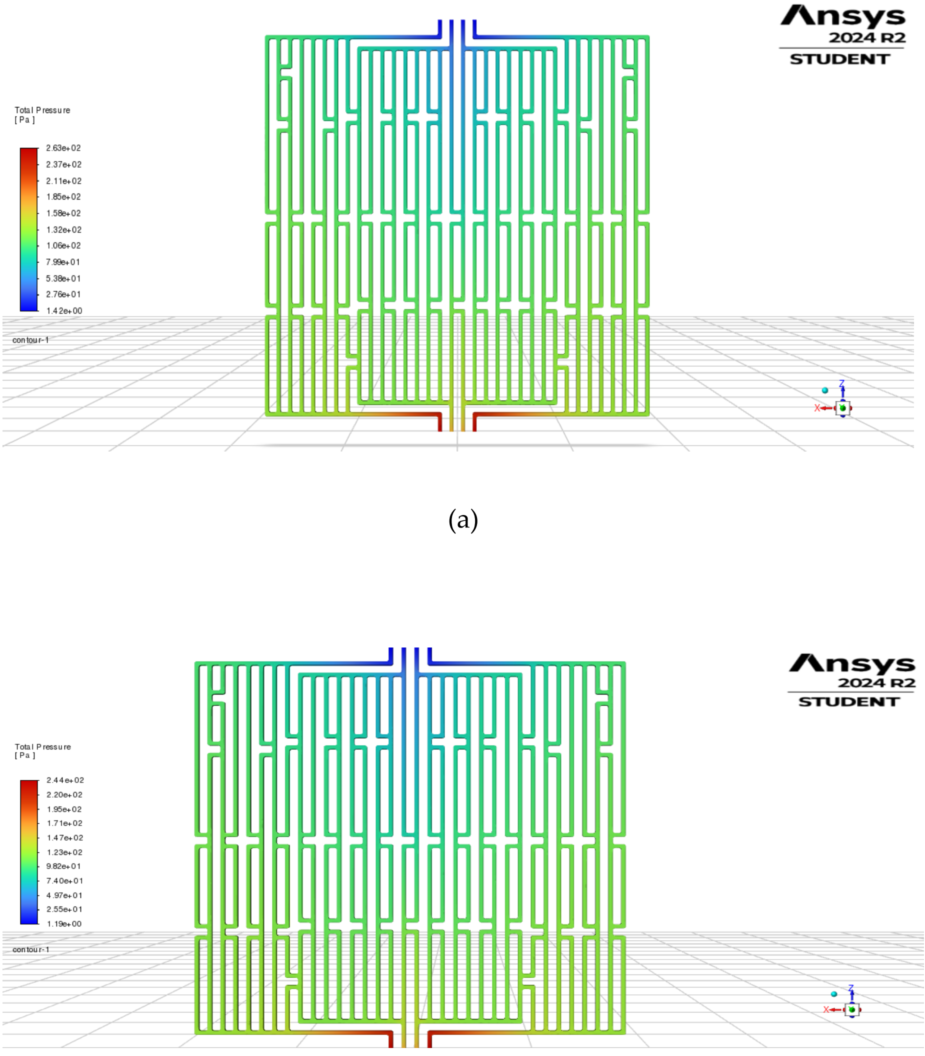

(a)

(b)

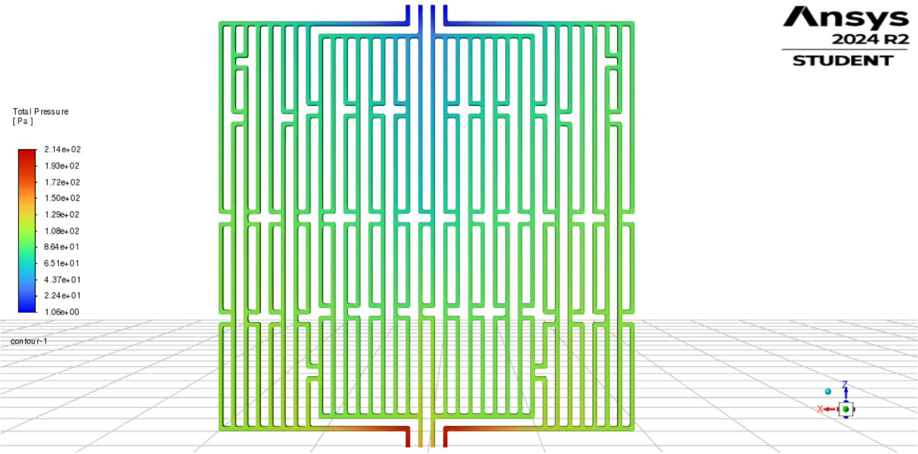
Total Pressure
[Pa]
2.14e+02
1.93e+02
1.72e+02
1.50e+02
1.29e+02
1.08e+02
8.64e+01
6.51e+01
4.37e+01
2.24e+01
1.06e+00
contour-1
Ansys
2024 R2
STUDENT
Z
X

(c)

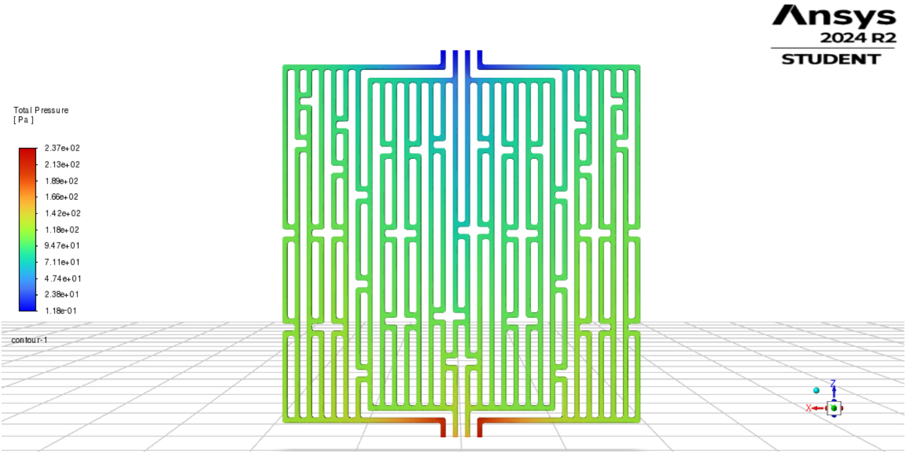
Total Pressure
[Pa]
2.37e+02
2.13e+02
1.89e+02
1.66e+02
1.42e+02
1.18e+02
9.47e+01
7.11e+01
4.74e+01
2.38e+01
1.18e-01
contour-1
Ansys
2024 R2
STUDENT
Z
X

(d)

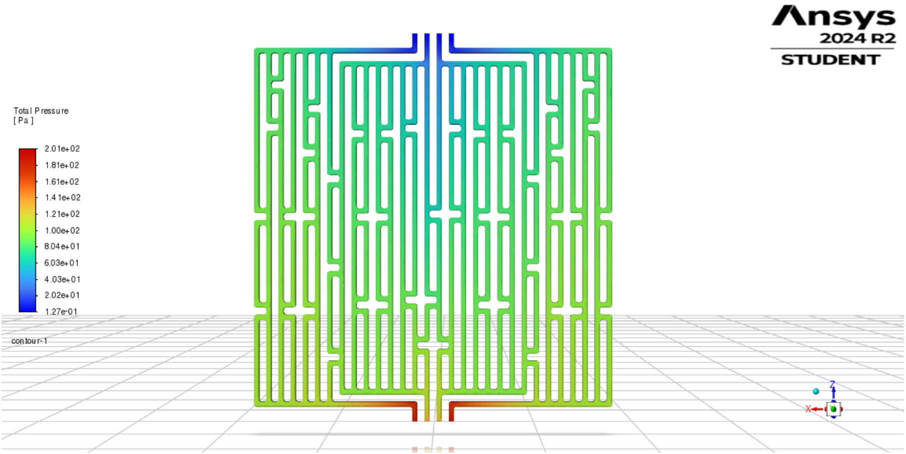
Total Pressure
[Pa]
2.01e+02
1.81e+02
1.61e+02
1.41e+02
1.21e+02
1.00e+02
8.04e+01
6.03e+01
4.03e+01
2.02e+01
1.27e-01
contour-1
Ansys
2024 R2
STUDENT
Z
X

(e)

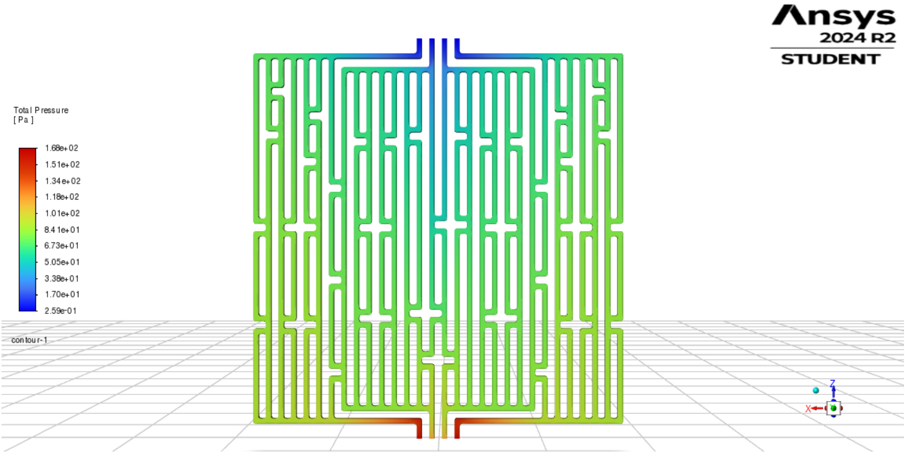
Ansys
2024 R2
STUDENT
Total Pressure
[Pa]
1.68e+02
1.51e+02
1.34e+02
1.18e+02
1.01e+02
8.41e+01
6.73e+01
5.05e+01
3.38e+01
1.70e+01
2.59e-01
contour-1
Z
X

(f)

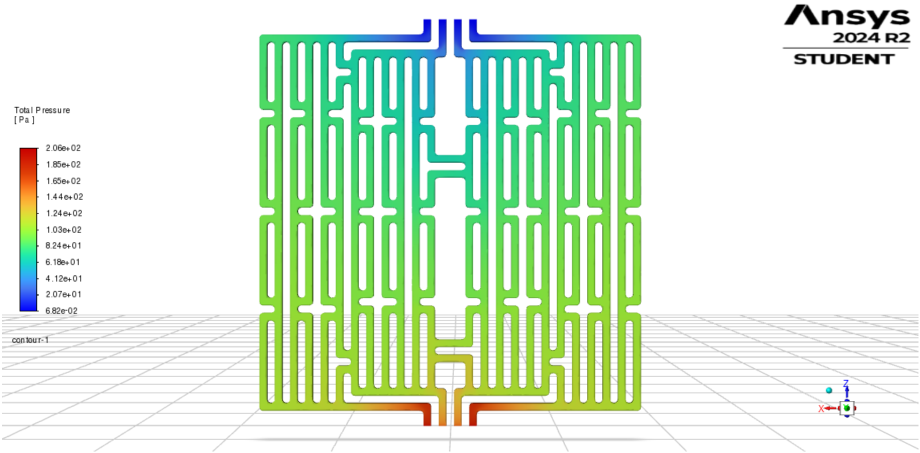
Ansys
2024 R2
STUDENT
Total Pressure
[Pa]
2.06e+02
1.85e+02
1.65e+02
1.44e+02
1.24e+02
1.03e+02
8.24e+01
6.18e+01
4.12e+01
2.07e+01
6.82e-02
contour-1
Z
X

(g)

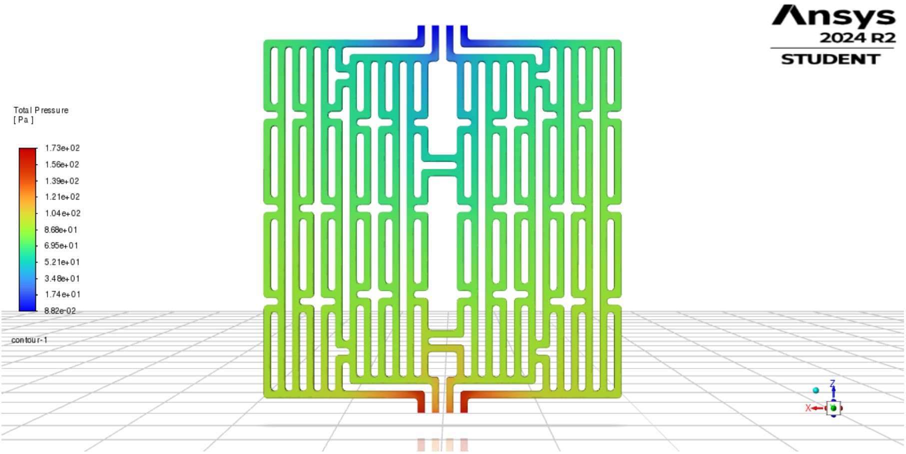
Ansys
2024 R2
STUDENT
Total Pressure
[Pa]
1.73e+02
1.56e+02
1.39e+02
1.21e+02
1.04e+02
8.68e+01
6.95e+01
5.21e+01
3.48e+01
1.74e+01
8.82e-02
contour-1
Z
X

(h)

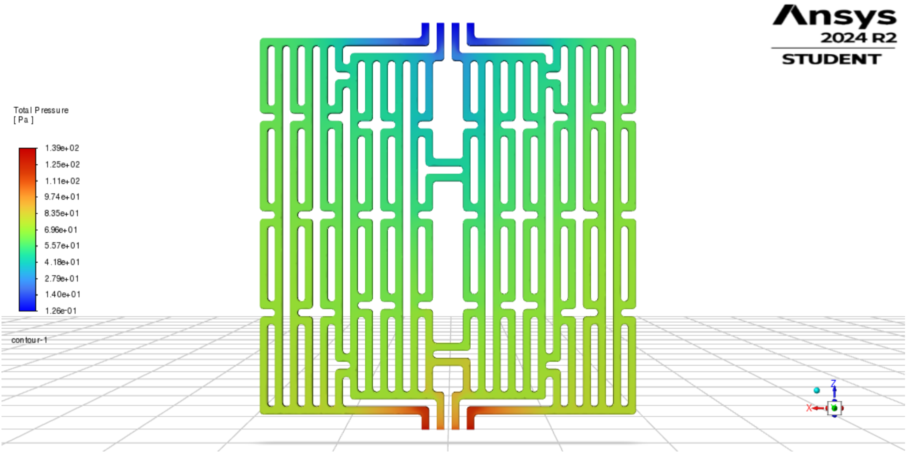

(i)

Figure 2. The hydrogen pressure distribution for all design variations using Ansys Simulation (a) PRL1, (b) PRL2, (c) PRL3, (d) PRL4, (e)PRL5, (f)PRL6, (g)PRL7, (h) PRL8, (i) PRL9

The CFD simulation results presented in Figure 2. demonstrate that variations in channel width and depth significantly influence the pressure drop within the modified parallel bipolar plates. The maximum pressure, initially at 263 Pa for a 0.5 mm channel width, decreases drastically with increasing channel width, reaching a minimum of 214 Pa after the addition of depth. This pressure drop is also observed in designs with 0.7 mm and 1 mm channel widths. A similar trend is evident with increasing channel width, where the initial maximum pressure of 264 Pa at 0.5 mm width decreases to 237 Pa at 0.7 mm width and further reduces to 206 Pa at 1 mm width.

Furthermore, the simulation results reveal that design variations impact the pressure distribution across different channel sections. Channels with multiple bends exhibit a more consistent pressure profile compared to those with fewer bends, as observed in the 0.7 mm and 1 mm width designs. The 1 mm wide channel only shows blue regions (low pressure) near the outlet, whereas in the 0.7 mm design, the low-pressure area is more extensive and extends towards the center.

These findings align with previous research. Wilberforce et al.[15] using a 5 x 5 cm^2 active area, observed a more stable pressure profile with gradual pressure drop in a parallel design incorporating serpentine adaptations. Similarly, Rosli et al.[16] demonstrated that bends or serpentine features in bipolar plate designs effectively reduce pressure and provide a more uniform pressure distribution. Their study showed that designs with bends have contour values below 1, indicating that water in the gas diffusion layer remains in vapor form, effectively mitigating flooding issues in parallel bipolar plates. Hu et al. [17] also showed that serpentine bend adaptations result in uniform pressure distribution and significantly enhance power density.

These findings align with previous research, particularly regarding the influence of bends within the flow channels. As demonstrated by previous research[15–17], channel bends can significantly affect pressure distribution. In the CFD simulations conducted here, the addition of bends also maintained a more stable pressure profile and distributed pressure more evenly, reducing the risk of flow maldistribution. The observed decrease in pressure with increasing channel width aligns with Chowdhury et al.[18], who investigated the influence of channel and land width using 19 variations and found a similar pressure reduction trend with increasing channel width.

3.3. Hydrogen Velocity Analysis using Computational Fluid Dynamics (CFD) Simulation

Figure 3 shows the influence of channel width and depth variations on hydrogen velocity.

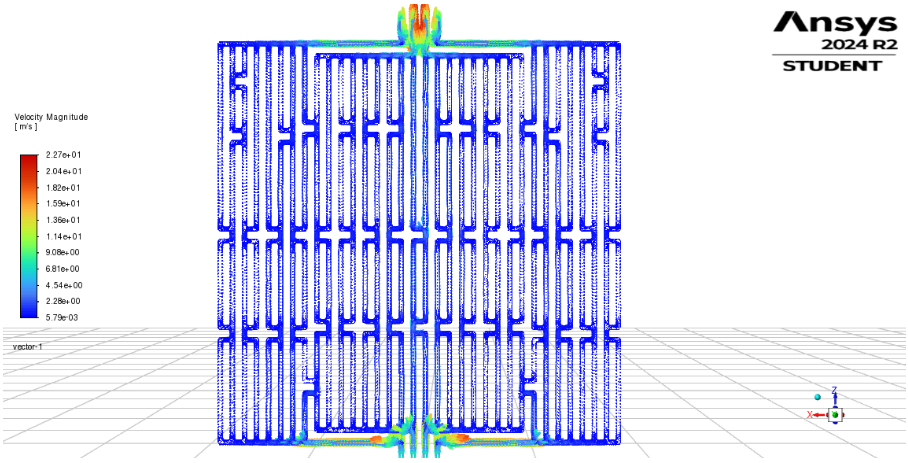

(a)

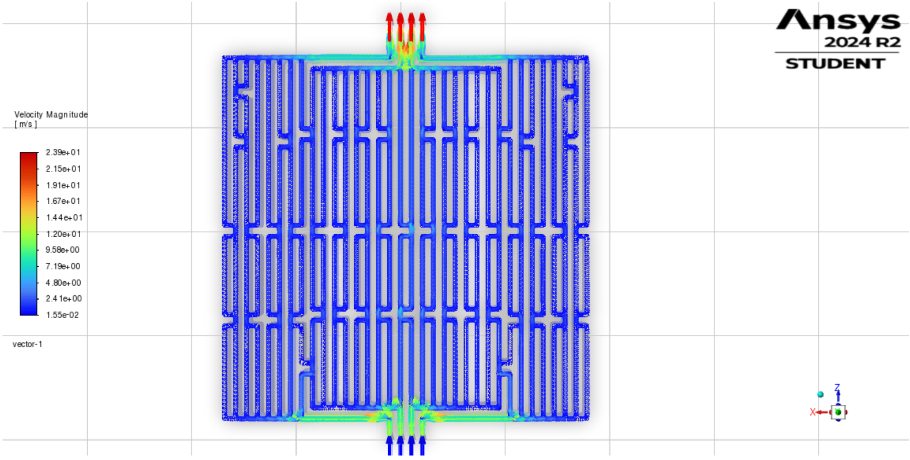

(b)

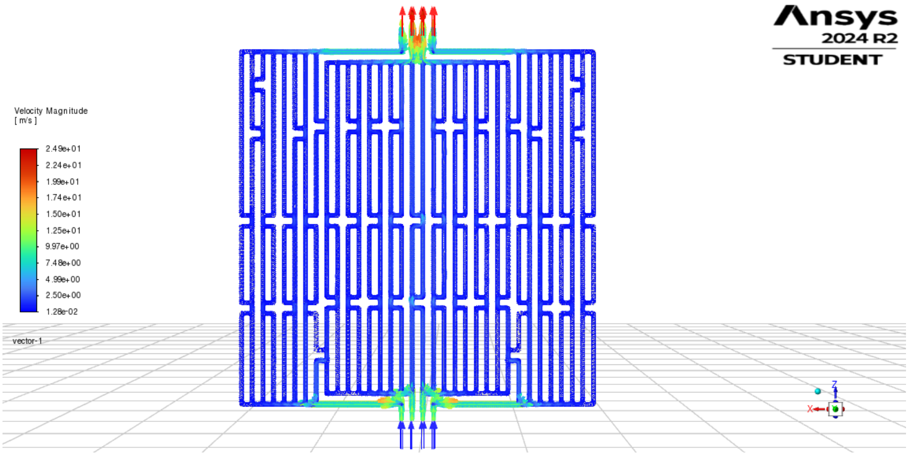
Velocity Magnitude
[m/s]
2.49e+01
2.24e+01
1.99e+01
1.74e+01
1.50e+01
1.25e+01
9.97e+00
7.48e+00
4.99e+00
2.50e+00
1.28e-02
vector-1
Ansys
2024 R2
STUDENT
Z
X

(c)

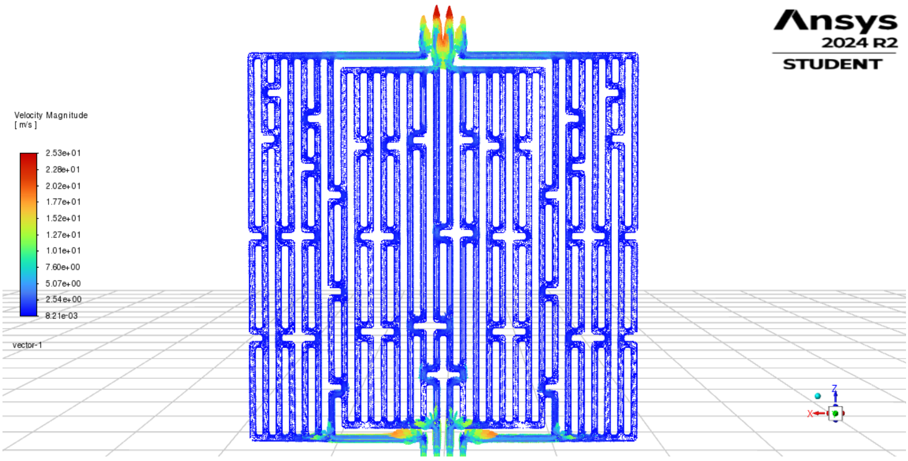
Velocity Magnitude
[m/s]
2.53e+01
2.28e+01
2.02e+01
1.77e+01
1.52e+01
1.27e+01
1.01e+01
7.60e+00
5.07e+00
2.54e+00
8.21e-03
vector-1
Ansys
2024 R2
STUDENT
Z
X

(d)

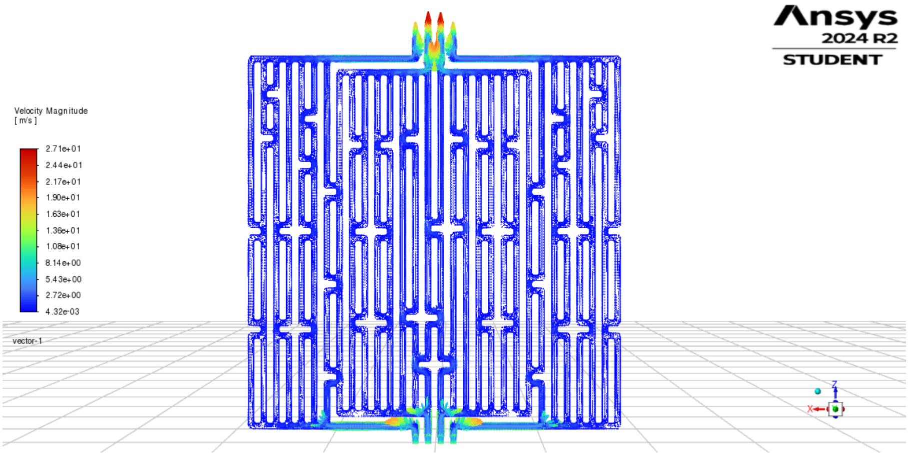
Velocity Magnitude
[m/s]
2.71e+01
2.44e+01
2.17e+01
1.90e+01
1.63e+01
1.36e+01
1.08e+01
8.14e+00
5.43e+00
2.72e+00
4.32e-03
vector-1
Ansys
2024 R2
STUDENT
Z
X

(e)

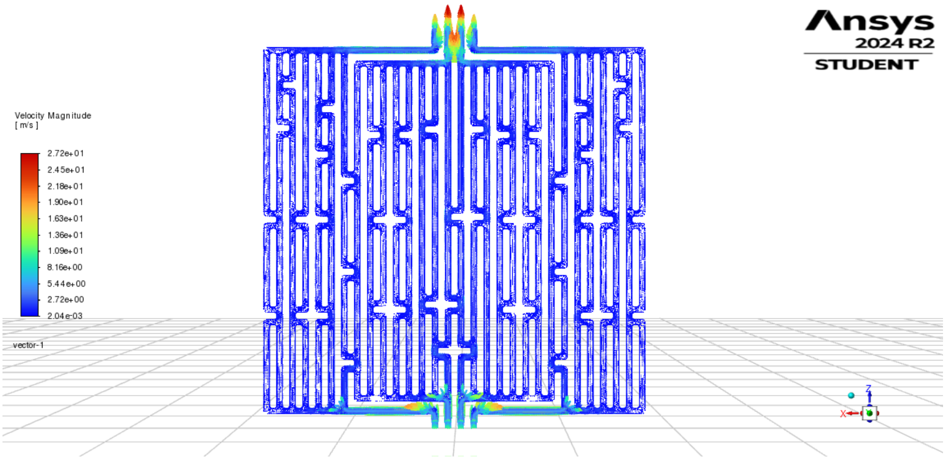
Velocity Magnitude
[m/s]
2.72e+01
2.45e+01
2.18e+01
1.90e+01
1.63e+01
1.36e+01
1.09e+01
8.16e+00
5.44e+00
2.72e+00
2.04e-03
vector-1
Ansys
2024 R2
STUDENT
Z
X

(f)

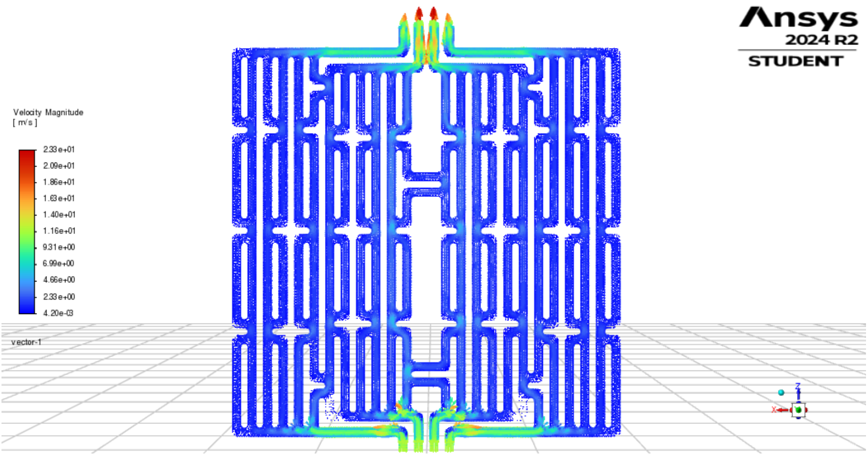
Velocity Magnitude
[m/s]
2.33e+01
2.09e+01
1.86e+01
1.63e+01
1.40e+01
1.16e+01
9.31e+00
6.99e+00
4.66e+00
2.33e+00
4.20e-03
vector-1
Ansys
2024 R2
STUDENT
Z
X

(g)

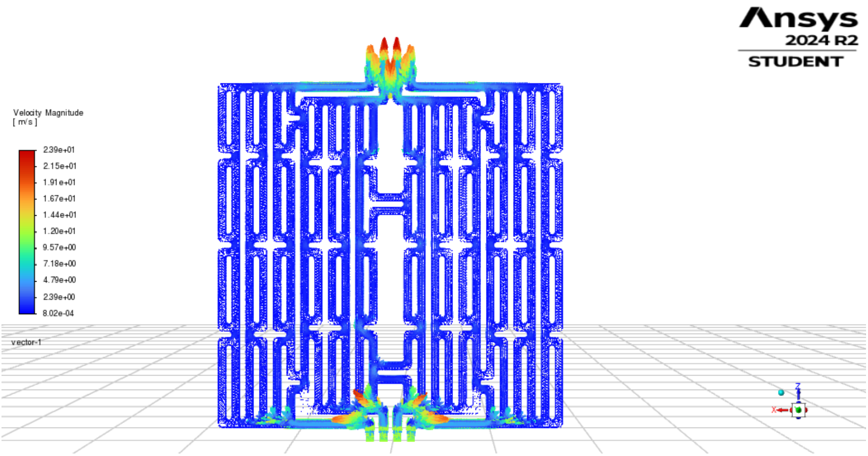
Velocity Magnitude
[m/s]
2.39e+01
2.15e+01
1.91e+01
1.67e+01
1.44e+01
1.20e+01
9.57e+00
7.18e+00
4.79e+00
2.39e+00
8.02e-04
vector-1
Ansys
2024 R2
STUDENT
Z
X

(h)

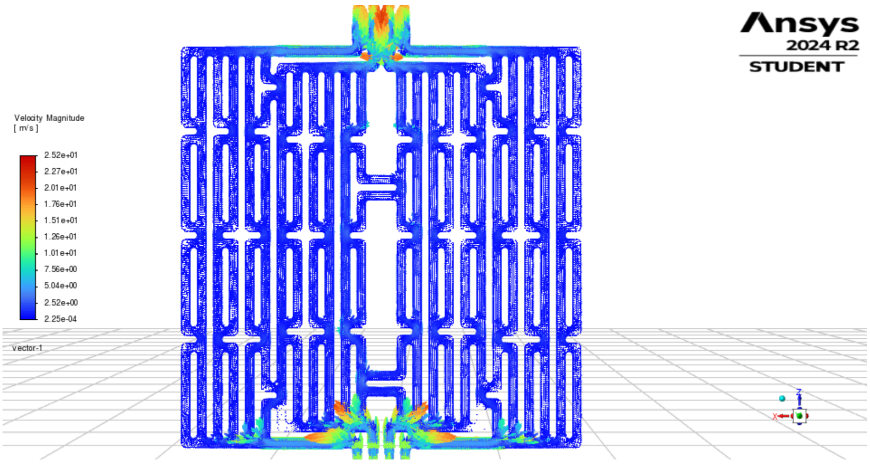

(i)

Figure 3. The hydrogen pressure distribution for all design variations using Ansys Simulation (a) PRL1, (b) PRL2, (c) PRL3, (d) PRL4, (e)PRL5, (f)PRL6, (g)PRL7, (h) PRL8, (i) PRL9

The CFD simulations illustrated in Figure 3. present results that are inversely related to the pressure values. While the pressure values obtained from the simulations decrease with increasing channel width, the CFD simulation results for hydrogen flow velocity show an increase.

At a width of 0.5 mm, the maximum hydrogen flow velocity is initially 22.7 m/s. This velocity increases to 23.9 m/s and reaches a peak of 24.9 m/s as the channel depth increases. A similar trend is observed in designs with widths of 0.7 mm and 1 mm. At a channel width of 0.7 mm, the maximum velocity obtained is 25.3 m/s, which increases with the addition of channel depth, peaking at 27.1 m/s. Meanwhile, at a width of 1 mm, the maximum velocity starts at 23.3 m/s but increases with the addition of depth, reaching a high of 25.2 m/s. Furthermore, increasing the channel width also shows a trend of increasing flow velocity. However, this does not apply when the channel width increases from 0.7 mm to 1 mm.

The CFD results also demonstrate the influence of hydrogen flow velocity on reactant gas distribution. At a channel width of 0.5 mm, the reactants are distributed evenly, but the gas flow velocity is very slow. At a channel width of 0.7 mm, the flow velocity increases, leading to improved reactant flow. However, this does not hold true for a channel width of 1 mm. Instead, a width of 1 mm results in uneven flow distribution (maldistribution) with flow concentration only in certain areas.

These findings are consistent with previous studies. Wang et al.[19] investigated the effect of outlet and inlet constriction and showed that areas with high pressure result in low gas flow velocity, and vice versa. Their design demonstrated increased gas flow velocity upon entering a small, low-pressure inlet. Liu et al.[20] studied the development of conventional designs by adding constrictions to parallel channels and showed that the pressure drop in sub-channels initially decreases and then increases with increasing distance. This study illustrated that pressure drop variation in sub-channels is a major contributor to flow maldistribution. Their design, incorporating micro-distributors, aimed to prevent excessive pressure drop in complex parallel channels and avoid excessively high pressure at the gas inlet path in the cathode. Flow maldistribution still occurred at sizes of 0.8 mm and 0.6 mm, while sizes of 0.4 mm and 0.2 mm showed significant pressure increases, reducing excessive pressure drop and improving flow distribution. Zhang et al. [21] conducted research on flow optimization in parallel designs and showed that increasing the number of branches in parallel channels leads to a decrease in the resulting flow velocity.

This study's results align with these previous findings. The CFD simulation results for larger channel widths and the associated pressure drop, which are closely related to flow distribution, show similarities to the findings of previous research[19,20], who identified high pressure and pressure drop as key factors in flow maldistribution in narrow and complex channel designs. Additionally, the observed increase in hydrogen flow velocity with increasing channel depth in this study mirrors the results of Zhang et al.[21], who observed a decrease in flow velocity with an increase in the number of branches in parallel channels.

4. Conclusions

Channel width and depth significantly influence the pressure distribution and hydrogen velocity in PEMFCs. Wider channel widths tend to decrease the maximum pressure, while deeper channel depths promote a more uniform pressure distribution across the bipolar plate. This suggests that optimizing both parameters is crucial for reducing pressure drop and achieving a more stable hydrogen flow rate

Author Contributions: "Conceptualization, V.R and M.N.; methodology, M.N., and V.N.G.; software, M.N. and R.M.; validation, V.R., and V.N.G.; formal analysis, V.R and M.N; writing—original draft preparation, M.N., V.N.G., and R.M.; writing—review and editing, V.R and M.N.; supervision, V.R. and R.M.; funding acquisition, V.R. All authors have read and agreed to the published version of the manuscript.

Conflicts of Interest: The authors declare no conflict of interest.

References

1. Soleimani, A.; Hosseini Dolatabadi, S.H.; Heidari, M.; Pinnarelli, A.; Mehdizadeh Khorrami, B.; Luo, Y.; Vizza, P.; Brusco, G. Progress in Hydrogen Fuel Cell Vehicles and Up-and-Coming Technologies for Eco-Friendly Transportation: An International Assessment. *Multiscale and Multidisciplinary Modeling, Experiments and Design* 2024, *7*, 3153–3172, doi:10.1007/s41939-024-00482-8.
2. Singla, M. Trends so Far in Hydrogen Fuel Cell Technology: State of the Art. *International Journal of Advanced Trends in Computer Science and Engineering* 2019, 1146–1155, doi:10.30534/ijatcse/2019/23842019.

3. Das, V.; Padmanaban, S.; Venkitusamy, K.; Selvamuthukumaran, R.; Blaabjerg, F.; Siano, P. Recent Advances and Challenges of Fuel Cell Based Power System Architectures and Control – A Review. *Renewable and Sustainable Energy Reviews* 2017, *73*, 10–18, doi:https://doi.org/10.1016/j.rser.2017.01.148.
4. Zainuri, F.; Hidayat Tullah, M.; Prasetya, S.; Susanto, I.; Purnama, D.; Subarkah, R.; Ramiati, T.; Widiyatmoko; Noval, R. Electric Vehicle Conversion Study for Sustainable Transport. *Recent in Engineering Science and Technology* 2023, *1*, 18–24, doi:10.59511/riestech.v1i02.15.
5. Porstmann, S.; Wannemacher, T.; Drossel, W.-G. A Comprehensive Comparison of State-of-the-Art Manufacturing Methods for Fuel Cell Bipolar Plates Including Anticipated Future Industry Trends. *J Manuf Process* 2020, *60*, 366–383, doi:https://doi.org/10.1016/j.jmapro.2020.10.041.
6. Wenkai, L.; Zhiyong, X.; Haodong, Z. Current Status of Research on Composite Bipolar Plates for Proton Exchange Membrane Fuel Cells (PEMFCs): Nanofillers and Structure Optimization. *RSC Adv* 2024, *14*, 7172–7194, doi:https://doi.org/10.1039/d3ra08054d.
7. Wu, S.; Yang, W.; Yan, H.; Zuo, X.; Cao, Z.; Li, H.; Shi, M.; Chen, H. A Review of Modified Metal Bipolar Plates for Proton Exchange Membrane Fuel Cells. *Int J Hydrogen Energy* 2021, *46*, 8672–8701, doi:https://doi.org/10.1016/j.ijhydene.2020.12.074.
8. Sauermoser, M.; Kizilova, N.; Pollet, B.; Kjelstrup, S. Flow Field Patterns for Proton Exchange Membrane Fuel Cells. *Front Energy Res* 2020, *8*, doi:10.3389/fenrg.2020.00013.
9. Jackson, J.M.; Hupert, M.L.; Soper, S.A. Discrete Geometry Optimization for Reducing Flow Non-Uniformity, Asymmetry, and Parasitic Minor Loss Pressure Drops in Z-Type Configurations of Fuel Cells. *J Power Sources* 2014, *269*, 274–283, doi:https://doi.org/10.1016/j.jpowsour.2014.06.136.
10. Zhang, Y.; Tu, Z. Flow-Field Design of the Bipolar Plates in Polymer Electrolyte Membrane Fuel Cell: Problem, Progress, and Perspective. *Applications in Energy and Combustion Science* 2024, *17*, 100244, doi:https://doi.org/10.1016/j.jaecs.2023.100244.
11. Imbrioscia, G.M.; Fasoli, H.J. Simulation and Study of Proposed Modifications over Straight-Parallel Flow Field Design. *Int J Hydrogen Energy* 2014, *39*, 8861–8867, doi:https://doi.org/10.1016/j.ijhydene.2013.11.079.
12. Xu, Y.; Peng, L.; Yi, P.; Lai, X. Analysis of the Flow Distribution for Thin Stamped Bipolar Plates with Tapered Channel Shape. *Int J Hydrogen Energy* 2016, *41*, 5084–5095, doi:https://doi.org/10.1016/j.ijhydene.2016.01.073.
13. Assagaf, I.; Sukandi, A.; Abdillah, A.A. Machine Failure Detection Using Deep Learning. *Recent in Engineering Science and Technology* 2023, *1*, 26–31.
14. Kahraman, H.; Orhan, M.F. Flow Field Bipolar Plates in a Proton Exchange Membrane Fuel Cell: Analysis & Modeling. *Energy Convers Manag* 2017, *133*, 363–384, doi:https://doi.org/10.1016/j.enconman.2016.10.053.
15. Wilberforce, T.; El-Hassan, Z.; Khatib, F.N.; Al Makky, A.; Mooney, J.; Barouaji, A.; Carton, J.G.; Olabi, A.-G. Development of Bi-Polar Plate Design of PEM Fuel Cell Using CFD Techniques. *Int J Hydrogen Energy* 2017, *42*, 25663–25685, doi:https://doi.org/10.1016/j.ijhydene.2017.08.093.
16. Rosli, M.; Lim, B.; Majlan, E.H.; Husaini, T.; Wan Daud, W.; Lim, S.F. Performance Analysis of PEMFC with Single-Channel and Multi-Channels on the Impact of the Geometrical Model. *Energies (Basel)* 2022, *15*, 7960, doi:10.3390/en15217960.
17. Hu, C.; Zhao, Y.; Zhang, Z.; Zhang, H.; Chen, D. Optimization of Flow Field Structure for Proton Exchange Membrane Fuel Cell Stack by Multi-Physics Coupling Simulation. *Int J Electrochem Sci* 2023, *18*, 100195, doi:https://doi.org/10.1016/j.ijoes.2023.100195.

18. Chowdhury, M.Z.; Genc, O.; Toros, S. Numerical Optimization of Channel to Land Width Ratio for PEM Fuel Cell. *Int J Hydrogen Energy* 2018, *43*, 10798–10809, doi:https://doi.org/10.1016/j.ijhydene.2017.12.149.

19. Wang, C.-C.; Yang, K.-S.; Tsai, J.-S.; Chen, I.Y. Characteristics of Flow Distribution in Compact Parallel Flow Heat Exchangers, Part I: Typical Inlet Header. *Appl Therm Eng* 2011, *31*, 3226–3234, doi:https://doi.org/10.1016/j.applthermaleng.2011.06.004.

20. Liu, H.; Yang, W.; Tan, J.; An, Y.; Cheng, L. Numerical Analysis of Parallel Flow Fields Improved by Micro-Distributor in Proton Exchange Membrane Fuel Cells. *Energy Convers Manag* 2018, *176*, 99–109, doi:https://doi.org/10.1016/j.enconman.2018.09.024.

21. Zhang, W.; Hu, P.; Lai, X.; Peng, L. Analysis and Optimization of Flow Distribution in Parallel-Channel Configurations for Proton Exchange Membrane Fuel Cells. *J Power Sources* 2009, *194*, 931–940, doi:https://doi.org/10.1016/j.jpowsour.2009.05.033.